

Auger Electron Cascades in Water and Ice

Nicușor Tîmneanu, Carl Caleman, Janos Hajdu,
David van der Spoel¹

*Department of Cell and Molecular Biology, Biomedical Centre, Box 596, Uppsala
University, SE-75124 Uppsala, Sweden*

Abstract

Secondary electron cascades can induce significant ionisation in condensed matter due to electron-atom collisions. This is of interest in the context of diffraction and imaging using X-rays, where radiation damage is the main limiting factor for achieving high resolution data. Here we present new results on electron-induced damage on liquid water and ice, from the simulation of Auger electron cascades. We have compared our theoretical estimations to the available experimental data on elastic and inelastic electron-molecule interactions for water and found the theoretical results for elastic cross sections to be in very good agreement with experiment. As a result of the cascade we find that the average number of secondary electrons after 100 fs in ice is about 25, slightly higher than in water, where it is about 20. The difference in damage between ice and water is discussed in the context of sample handling for biomolecular systems.

Key words: Photoelectric effect, Auger decay, X-ray Free Electron Laser, Diamond, Ice, Water

¹ email: spoel@xray.bmc.uu.se

1 Introduction

High energy X-rays damage matter, mainly through the photoelectric effect. A photon is absorbed by an atom and a photoelectron is emitted from the inner (K) shell of the atom. In biological molecules, the remaining hollow ion might relax through Auger decay, in which an electron from a higher level falls down and a further electron is emitted with an energy between 250 eV and 2 keV [1]. The basic atomic physics for these processes is well understood and cross sections for photoionization have been tabulated [2,3]. Furthermore, Auger line widths have been measured giving K-hole life times, of *e.g.* 11.1 fs (C), 9.3 fs (N), 6.6 fs (O) and 1.3 fs (S) [4]. During the photoionization process, the photoelectron may interact with electrons in the valence shell. For elements of biological significance this may lead to the so called shake-up and shake-off effects [5] in which a further low energy electron (10-100 eV) is emitted. Semi-empirical quantum calculations were used to estimate that such shake-off ionizations occur in 10 - 30% events [6].

The advent of X-ray free electron lasers (FEL) will enable a whole range of new experiments in physics, chemistry and biology within a few years [7,8,9]. In the category of biological applications, we envision performing structural studies on large biomolecules, biomolecular aggregates or nanocrystals. Molecular dynamics simulations of a protein molecule in a FEL beam are encouraging as to the feasibility of such experiments [10]. Preliminary studies with a simple hydrodynamic model have suggested that [11] a layer of water or ice may delay the eventual Coulomb explosion of a biomolecule, such as a protein, in a FEL beam [10]. The reason for this is that water molecules at the surface supply electrons to neutralize the charging core of the droplet, where the protein is expected to be situated, while protons, carrying the positive charge, are expelled from the water shell. This may be advantageous in future experiments if the sample is held in water droplets.

In the aftermath of a photoionization event in a liquid or solid, further electrons will be liberated through collisions between the Auger electron and the atoms, leading to a cascade of ionizations. Recent studies [12,13] have made a critical assessment of the total amount of electrons due to an Auger electron of 250 eV (carbon)². It was predicted that in diamond, between 6 and 13 electrons will be released, while for amorphous carbon the number is somewhat higher due to the absence of a band gap [12]. Here we present results on water, both in liquid and solid state. The understanding of Auger electron cascades in water is essential for modeling the shielding effects water molecules will have on *e.g.* a protein sample. Furthermore, water is less dense than diamond

² Although the actual Auger energy for carbon in diamond is 265 eV [14], we have used the value of 250 eV for comparison with earlier work.

and therefore more comparable to biomolecules. The Auger electron energy for oxygen in a water molecule is 507.9 eV [15], providing twice as much energy to the electron than carbon.

2 Theory

To calculate the cross sections for scattering of electrons on atoms used in the molecular dynamics model, we have used a solid state approach, assuming a neutral crystal, or, in the case of liquid water, a neutral cluster with periodic boundary conditions. The same approach has been used earlier by Ziaja *et al.* [12,13]. Under this assumption, there are three different interactions that a free electron in the medium can undergo: (i) elastic collision with atoms, (ii) inelastic collision with atoms or (iii) recombination with atoms or ions. The probability of electron-ion recombination is low on the time scale considered here ($t \sim 100$ fs) and therefore neglected [16]. Inelastic collision of electrons with ions are not considered, since the number of ionizations caused by a photoelectron or single primary Auger electron is much smaller than the total number of atoms in the sample. Scattering of electrons on phonons and the vibrational cross section are not considered here, though they become relevant for low energies ($E \leq 10$ eV) [17].

Elastic scattering

The cross section for the elastic scattering of electrons on atoms is calculated using programs from the Barbieri/van Hove Phase Shift package [18]. The calculations are based on the partial wave expansion technique, using the muffin-tin potential approximation. The expression for the elastic cross section as a function of the electron energy E , is

$$\sigma_{\text{elastic}}(E) = \frac{2\pi\hbar^2}{Em_e} \sum_l (2l+1) \sin^2 \delta_l, \quad (1)$$

where δ_l is the phase shift of each partial wave l . For further details on the elastic cross section calculations see reference [13] and references therein.

The energy of an elastically scattered electron is conserved, and the only effect the collision has on the system is that the direction of the electron velocity changes. For the calculations of the cross sections in liquid water we have used a unit cell with hydrogen bonded water molecules at liquid density (0.9965 g/cm^3), while for ice calculations we have used hexagonal ice, I_h (density 0.9197 g/cm^3). The results of our calculations are shown in Fig. 1

together with results for diamond [13]. The results compare very well with the experimental data for electron scattering on water molecules.

Inelastic scattering

A correct treatment of the inelastic scattering is more complicated and, to our knowledge, there is no complete method to describe this. We followed the approach presented in our previous work [13]. We have used two different optical data models, the Ashley model [21,22] and the Tanuma, Powell and Penn model (TPP2) [23,24], together with the Lindhard dielectric function $\varepsilon(q, \omega)$ [25,26,27] for the calculations of the inelastic cross section

$$\sigma_{\text{inelastic}}(E) \sim \frac{1}{E} \int_0^\infty d\omega \int_{q_-}^{q_+} \frac{dq}{q} \text{Im} \left(\frac{-1}{\varepsilon(q, \omega)} \right), \quad (2)$$

were $\hbar q_{\pm} = \sqrt{2m_e} (\sqrt{E} \pm \sqrt{E - \hbar\omega})$. The above cross section depends on the knowledge of the dielectric function, which is only known for photons, *i.e.* for momentum transfer equal to zero. The two different models, Ashley and TPP2, present different ways to empirically compensate for that. The Ashley approach includes the exchange between the incoming electron and the electrons in the crystal, in accordance with the non relativistic Møller cross section [28]. The TPP2 model is developed for calculating the differential inelastic mean free path of electrons in a solid. A more thorough discussion of the two models can be found in ref. [13]. From the absorption coefficient for liquid water [29], we deduced the dielectric function $\varepsilon(0, \omega)$ for zero momentum transfer. For ice we used experimental data [30] for energies up to 30 eV, and for higher energies we have extrapolated the values assuming the shape of the curve to be the same as for liquid water (Fig. 2).

An electron that scatters inelastically will change its path and loose energy to the lattice and, if the lost energy is high enough to excite a bound electron from the valence band to the conduction band, to the excited electron. For simplicity we assumed that the energy lost to the lattice is absorbed into the system and in the present study we have not included any treatment for holes. The band gaps of water and ice we have used for the calculations were $E_{\text{gap}}^{\text{water}} = 8.7$ eV [31] and $E_{\text{gap}}^{\text{ice}} = 7.8$ eV [32]. For water the Fermi level $E_{\text{F}}^{\text{water}} = 14.85$ eV is taken from experimental data [31], and for ice $E_{\text{F}}^{\text{ice}} = 11.74$ eV was calculated using the free electron approximation with the density taken from reference [33]. The calculations were performed at temperature $T_{\text{ice}} = 270$ K and $T_{\text{water}} = 300$ K. The inelastic cross sections for ice and water are shown in Fig. 3 together with those from diamond, taken from reference [13].

From the wealth of experimental data for electron impact ionization of atoms and molecules, models and recommended cross sections have emerged for different targets. We have compared the theoretical estimates for inelastic scattering of electrons in solids (diamond, ice), with the recommended cross sections for carbon [34] and a successful model that describes ionization of water molecules [35] (Fig. 4). The former represent a fit to the atomic data for several light atoms and ions [34], while the latter, known as the Binary-Encounter-Bethe (BEB) model, provides analytical formulae for the ionization cross section of atomic and molecular orbitals by summing up all contributions. The BEB model was found to reproduce experimental data for small atoms and a variety of molecules very well [35].

We find that, in the case of diamond, the inelastic cross section is lower than the ionization of single atoms, reflecting the nonlocalized nature of the electrons in the solid. This difference could prove significant for the estimation of electron interaction in solids, if the solid loses its crystalline structure (due to Coulomb explosion while exposed to a FEL beam). For ice and water, however, we find a smaller difference between the ionization cross sections [35] and our theoretical estimates (Fig. 4), and with the opposite sign.

3 Methods

Classical simulations of the electron trajectories were performed, where Newton's equations of motion were solved using a Leap-Frog integration scheme [36] with a time step of $\Delta t = 1$ attoseconds. The lattice, be it diamond, water or ice, was modeled implicitly through the cross sections for collisions. Elastic as well as inelastic collisions were modeled as stochastic processes, where the probability $P(E)$ for an event was determined from:

$$P(E) = \frac{\rho N_{\text{av}}}{m} \sigma(E) \cdot |v_e(E)| \cdot \Delta t, \quad (3)$$

where ρ is the density of the material, N_{av} is Avogadro's number, m is the mass of the atom (C in diamond), respectively water molecule, and v_e is the velocity of the electron. Δt was chosen such that $P \ll 1$ in all cases. At each time step in the simulation the following processes occur:

(1) An electron with a certain kinetic energy E_k travels through the sample. The scattering probability (both inelastic and elastic) $P(E_k)$ is compared to a random number $0 \leq r < 1$. If no scattering occurs, the velocity is kept unchanged.

(2a) If the electron scatters elastically it changes its momentum according to a probability function derived from the differential cross section (the formulae in [13] were applied for water and ice). No momentum transfer to the lattice

has been considered at this point.

(2b) In the case of inelastic scattering, the electron will lose energy E_{lost} and change its path. If $E_{\text{lost}} > E_{\text{gap}}$ an additional electron is liberated from the valence band with $E_k = E_{\text{lost}} - E_{\text{gap}}$. If $E_{\text{lost}} < E_{\text{gap}}$, the energy is transferred to the lattice. In both cases the momentum is changed based on the differential cross section calculated for water and ice using formulae from [13].

(3) The electron position is integrated.

The spatial electron dynamics program is part of the GROMACS software package [37].

4 Results and Discussion

The classical dynamics simulations of the electrons produced the same results for diamond as our earlier Monte Carlo simulations [12], showing that the implementation of the algorithm is correct, and that the integration time step was small enough. In principle, the model could be enhanced by adding electrostatic interactions between electrons and ions [38]. It is however not trivial to model the interactions between electrons and ions classically without severe approximations. Since we have only simulated single Auger electron trajectories, and the cross sections were determined for neutral systems, we have deemed it unnecessary to add the Coulomb term. Finally, we note that correct treatment of electron/ion or electron/hole systems can be performed using *e.g.* time-dependent density functional calculations, but it is complicated, and not computationally feasible for macroscopic systems [39].

Ionization rates

We find that an Auger electron of 500 eV will produce typically between 5 and 10 secondary electrons in the first femtosecond in ice and water, a result which is comparable with the average number of ionization events in diamond from a 250 eV Auger electron. In ice and water, however, saturation appears much later, after about 100 fs, when the average number of ionizations is around 20 for liquid water and 25 for ice. These results are shown in Fig. 5, which not only compares the ionization rates for ice, water and diamond, but also shows that the simulation of diamond using classical dynamics reproduces previous results obtained with a Monte Carlo method well [12]. We note that, although the cross sections for ice and water are rather similar, the difference in the number of ionizations in the Auger electron cascade is determined mainly by the approximately 1 eV difference in the band gap between liquid water and ice.

Energy distribution

The total energy of the electrons shows a substantial drop during the first 10 femtoseconds, with the rest of the energy being transferred to the lattice (Fig. 6). The electron gas is cooling down very rapidly, due to the large number of ionizations, and the average temperature of the electrons kT_{el} is similar for ice and water. The energy lost to the lattice is more than 50% of the initial Auger electron energy. For comparison, the results obtained for diamond are also shown, consistent with the previous calculations [12].

The electron energy distribution as a function of time in the cascade (Fig. 7) is particularly interesting. In the early stages of the cascade (of the order of 0.1 fs), the electron population is divided in two sets, initial Auger electrons which are highly energetic (450-500 eV) and the first secondary electrons of lower energy. At the critical time of about 1 fs, the population of high energy electrons fades away, leaving a spread of electrons with intermediate and low energies. Subsequent collisions will cool down the electron gas very fast, and after 10 fs all the electrons will have energies less than 20 eV. At such low energies (below 10 eV) and long time scales (100-1000 fs), new processes become relevant, such as electron-ion recombination or electron-phonon scattering, which are not yet included in our model.

Spatial distribution

We have performed an analysis of spatial distribution of electrons in the cascade in our classical dynamics model for ice, water and diamond. Fig. 8 shows the average gyration radius of the electron cloud for ice, water and diamond. The spatial extension of the cloud in ice and water is three times larger than the one in diamond, due to the considerably lower density and the corresponding longer mean free path an electrons in water/ice.

5 Conclusion

An understanding of the behaviour of water and ice exposed to an intense X-ray beam is important for planned biology experiments with FELs. Biological macromolecules carry about 30-60% water with them as structural water and water bound as a surface layer. In the light of results from a hydrodynamic model [11], it was suggested that embedding a sample in water or ice may be beneficial in the sense that the eventual Coulomb explosion [10] could be delayed by the presence of the water or ice layer. Our results show that in

hexagonal ice, I_h , a slightly higher number of secondary electrons are liberated as compared to water (Fig. 5), despite the slightly lower temperature. Furthermore, the electrons are spread over a larger volume (Fig. 8). Although the differences are small, it seems therefore that water is the preferred medium for encapsulating biomolecules when studied in FEL beams. If the sample is embedded in vitreous ice, which could be true in case of a rapid freezing, we expect the behaviour to be unaffected compared to water.

Acknowledgments

We would like to thank Beata Ziaja, Magnus Bergh, Jorge Llano, Lars Nordström, Richard London, Gyula Faigel and Zoltán Jurek for stimulating discussions. The Swedish research foundation is acknowledged for financial support.

References

- [1] A. C. Thompson, D. Vaughan (Eds.), X-ray Data Booklet, 2nd Edition, Lawrence Berkeley National Laboratory, Berkeley, 2001.
- [2] W. J. Veigele, Photon cross sections from 0.1 keV to 1 MeV for elements with $Z=1$ to $Z=94$, Atomic Data 5 (1973) 51–111.
- [3] J. H. Hubbell, W. J. Veigele, E. A. Briggs, R. T. Brown, D. T. Cromer, R. J. Howerton, Atomic form factors, incoherent scattering functions, and photon scattering cross sections, J. Phys. Chem. Ref. Data 4 (1975) 471–494.
- [4] M. O. Krause, J. H. Oliver, Natural width of atomic K and L level $K\alpha$ X-ray lines and several KLL Auger lines, J. Phys. Chem. Ref. Data 8 (1979) 329–338.
- [5] K. Siegbahn, C. Nordling, G. Johansson, J. Hedman, P. H. Heden, K. Hamrin, U. Gelius, T. Bergmark, L. O. Werme, R. Manne, Y. Bear, ESCA applied to free molecules, North Holland, Amsterdam, 1969.
- [6] P. Persson, S. Lunell, A. Szöke, B. Ziaja, J. Hajdu, Shake-up and shake-off excitations with associated electron losses in x-ray studies of proteins, Prot. Sci. 10 (2001) 2480–2484.
- [7] B. H. Wiik, The TESLA project: an accelerator facility for basic science, Nucl. Inst. Meth. Phys. Res. B 398 (1997) 1–8.
- [8] J. Hajdu, K. Hodgson, J. Miao, D. van der Spoel, R. Neutze, C. V. Robinson, G. Faigel, C. Jacobsen, J. Kirz, D. Sayre, E. Weckert, G. Materlik, A. Szöke, Structural studies on single particles and biomolecules., in: LCLS: The First Experiments, SSRL, SLAC, Stanford, USA, 2000, pp. 35–62.

- [9] H. Winick, The linac coherent light source (LCLS): A fourth-generation light source using the SLAC linac, *J. Elec. Spec. Rel. Phenom.* **75** (1995) 1–8.
- [10] R. Neutze, R. Wouts, D. van der Spoel, E. Weckert, J. Hajdu, Potential for biomolecular imaging with femtosecond x-ray pulses, *Nature* **406** (2000) 752–757.
- [11] R. London, Private communication.
- [12] B. Ziaja, A. Szöke, D. van der Spoel, J. Hajdu, Space-time evolution of electron cascades in diamond, *Phys. Rev.* **B** (2002) 024116.
- [13] B. Ziaja, D. van der Spoel, A. Szöke, J. Hajdu, Radiation induced electron cascade in diamond and amorphous carbon, *Phys. Rev.* **B** **64** (2001) 214104.
- [14] F. Yue, R. S. Swineford, D. P. Pappas, Atomic-structure determination of diamond using auger-electron diffraction, *Phys. Rev.* **B** **53** (12) (1996) 8036–8041.
- [15] C. D. Wagner, D. A. Zatko, R. H. Raymond, Use of the oxygen KLL Auger lines in identification of surface chemical states by electron spectroscopy for chemical analysis, *Anal. Chem.* **52** (9) (1980) 1445–1451.
- [16] L. D. Landau, E. M. Lifschitz, *Quantum Mechanics (Non-relativistic Theory)*, 3rd Edition, Pergamon Press, Oxford, 1977.
- [17] M. Michaud, A. Wen, L. Sanche, Cross sections for low-energy (1-100 eV) electron elastic and inelastic scattering in amorphous ice, *Radiation Research* **159** (2003) 3–22.
- [18] A. Barrieri, M. A. van Hove, private communications; phase shift package, <http://electron.lbl.gov/leedpack>.
- [19] A. Danjo, H. Nishimura, Elastic scattering of electrons from H₂O molecule, *J. Phys. Soc. Jpn* **54** (4) (1985) 1224–1227.
- [20] A. Katase, K. Ishibashi, Y. Matsumoto, T. Sakae, S. Maezono, E. Murakami, K. Watanabe, H. Maki, Elastic scattering of electrons by water molecules over the range 100-1000 eV, *J. Phys.* **B** **19** (1986) 2715–2734.
- [21] J. C. Ashley, Energy loss rate and inelastic mean free path of low-energy electrons and positrons in condensed matter, *J. Electron Spectrosc. Relat. Phenom* **50** (1990) 323–334.
- [22] J. C. Ashley, Energy-loss probabilities for electrons, positrons, and protons in condensed matter, *J. Appl. Phys* **69** (2) (1991) 674–678.
- [23] D. R. Penn, Electron mean free paths for free-electron-like materials, *Phys. Rev.* **B** **13** (1976) 674.
- [24] S. Tanuma, C. J. Powell, D. R. Penn, Calculations of electron inelastic mean free paths for 31 materials, *Surf. Interface Anal.* **11** (1988) 577–589.
- [25] E. Fermi, *Z. Phys.* **29** (1924) 315.

- [26] H. Bethe, Zur theorie des durchgangs schneller korpuskularstrahlen durch materie, *Ann. Phys.* 5 (1930) 325–400.
- [27] J. Lindhard, *K. Dan. Vidensk. Selsk. Mat. Fys. Medd.* 28 (1954) 1.
- [28] M. Kaku, *Quantum Field Theory*, Oxford University Press, New York, 1993.
- [29] E. D. Palik (Ed.), *Handbook of Optical Constants of Solids II*, Academic Press, New York, 1991.
- [30] S. G. Warren, Optical constants of ice from the ultraviolet to the microwave, *Appl. Opt.* 23 (8) (1984) 1206–1225.
- [31] T. Shibaguchi, H. Onuki, R. Onaka, Electronic structures of water and ice, *J. Phys. Soc. Jpn* 42 (1) (1977) 152–158.
- [32] V. F. Petrenko, I. A. Ryzhkin, Electron energy spectrum of ice, *Phys. Rev. Lett.* 71 (16) (1993) 2626–2629.
- [33] K. Röttger, A. Endriss, J. Ihringer, Lattice constants and thermal expansion of H₂O and D₂O ice Ih between 10 and 265 K, *Acta Cryst B* 50 (6) (1994) 644–648.
- [34] K. L. Bell, H. G. Gilbody, J. G. Hughes, A. E. Kingston, F. J. Smith, Recommended data on electron impact ionization of light atoms and ions, *J. Phys. Chem. Ref. Data* 12 (4) (1983) 891–915.
- [35] Y.-K. Kim, M. Rudd, Binary-encounter-dipole model for electron-impact ionization, *Phys. Rev. B* 50 (5) (1994) 3954–3967.
- [36] H. J. C. Berendsen, W. F. van Gunsteren, Practical algorithms for dynamics simulations, in: G. Ciccotti, W. G. Hoover (Eds.), *Molecular-Dynamics Simulation of Statistical-Mechanical Systems*, North-Holland, Amsterdam, 1986, pp. 43–65.
- [37] E. Lindahl, B. A. Hess, D. van der Spoel, Gromacs 3.0: A package for molecular simulation and trajectory analysis, *J. Mol. Mod.* 7 (2001) 306–317.
- [38] Z. Jurek, G. Faigel, M. Tegze, Dynamics in a cluster under the influence of intense femtosecond hard X-ray pulses, [arXiv:physics/0306102](https://arxiv.org/abs/physics/0306102).
- [39] M. A. L. Marques, A. Castro, A. Rubio, Assessment of exchange-correlation functionals for the calculation of dynamical properties of small clusters in time-dependent density functional theory, *J. Chem. Phys.* 115 (7) (2001) 3006–3014.

Figure captions

- (1) Elastic cross sections for scattering of electrons on ice, water and diamond. Lines represent the scattering cross section per scattering center, derived using the Barbieri/van Hove Phase Shift method [18], for ice (full line) and water (dashed line). For comparison, the cross section for diamond taken from [13] is shown (dotted line). The experimental points represent the elastic scattering of electrons on water molecules as measured in [19,20].
- (2) The imaginary part of the inverse dielectric function, $\text{Im}(-1/\varepsilon(0, E))$, for water and ice plotted as a function of the incoming photon energy.
- (3) Inelastic cross section for electron scattering on ice and water as a function of the electron energy. Lines represent the cross section per scattering center, calculated using two optical data models, the Ashley model [21,22] and the Tanuma, Powell and Penn model (TPP2) [23,24]. For comparison, the cross sections for diamond taken from [13] are also shown.
- (4) Comparison between the inelastic cross section for electron scattering on solids (ice and diamond) and the ionization cross section for electron scattering on single atoms and molecules. Lines represent the calculated cross section using TPP2 model [23,24] for diamond (solid line) and ice (dashed line). Points represent the recommended cross section for carbon atoms [34] (solid points), and the calculated cross section Binary-Encounter-Bethe (BEB) model [35] for ionization of water molecules (circles).
- (5) Average number of secondary electrons as a function of time, from an initial Auger electron (at time $t=0$ fs) in ice (solid line), water (dashed line) and diamond (dotted line). Lines correspond to calculations using Ashley's model [21,22].
- (6) Average energy of the free electrons in an electron cascade coming from an initial Auger electron in ice and water as a function of time (thin lines). The rest of the Auger electron energy is transferred to the lattice. Average temperature kT_{el} of the electron gas versus time (thick lines) for water and diamond.
- (7) Histogram of the energy distribution $N(E, t)/N(t)$ among electrons at different time steps in ice. At a fixed time, the histogram is normalized to the number of electrons in the cascade $N(t)$. Results are shown for an average cascade produced by an Auger electron in ice.
- (8) The gyration radius (average distance of electrons from the cloud center of mass) of the electron cascade as a function of time, for ice, water and diamond.

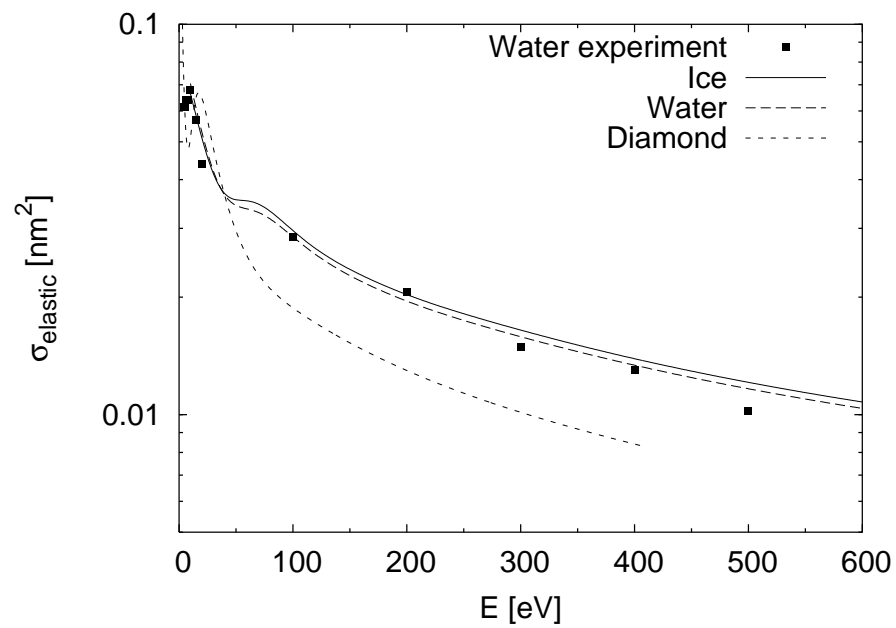


Fig. 1. Timneanu et al.

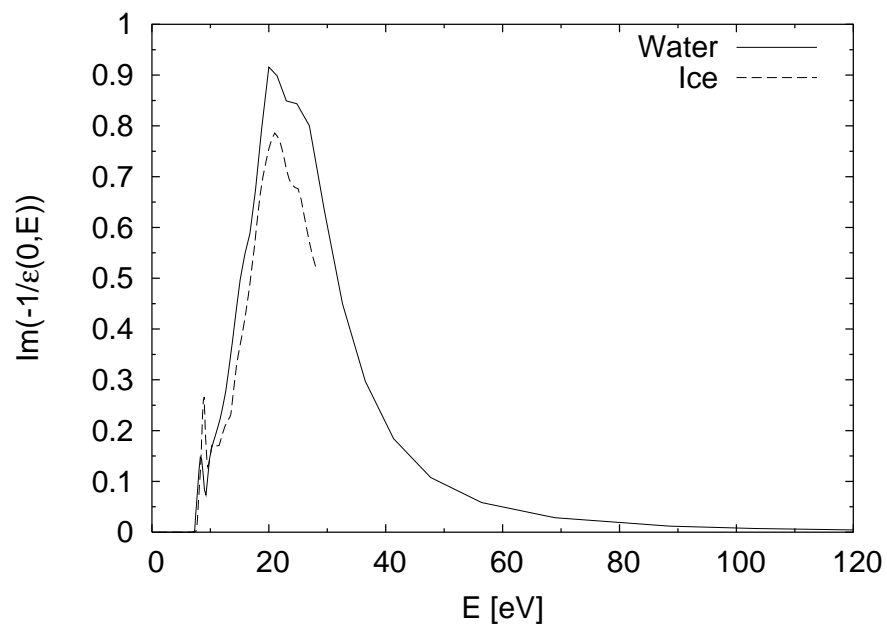


Fig. 2. Timneanu et al.

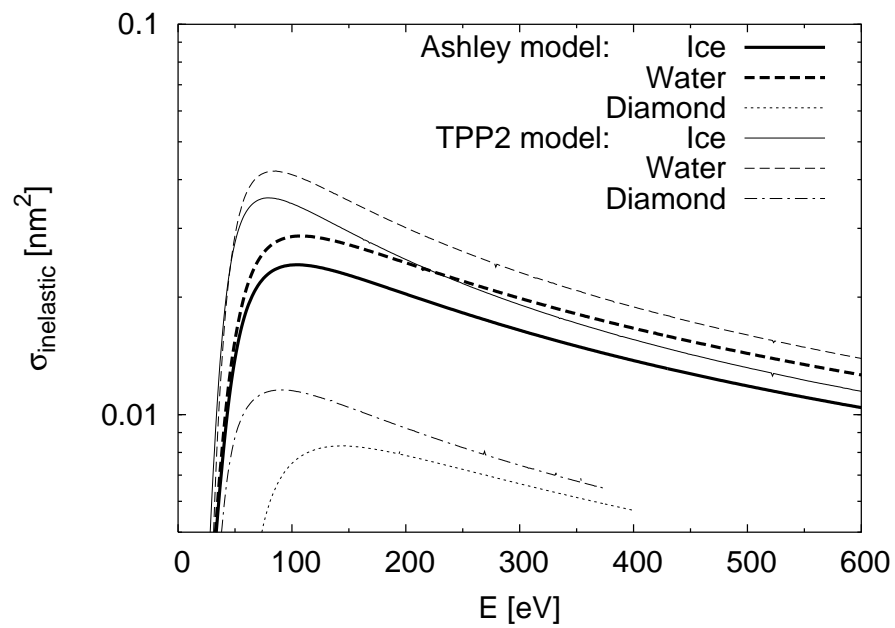


Fig. 3. Timneanu et al.

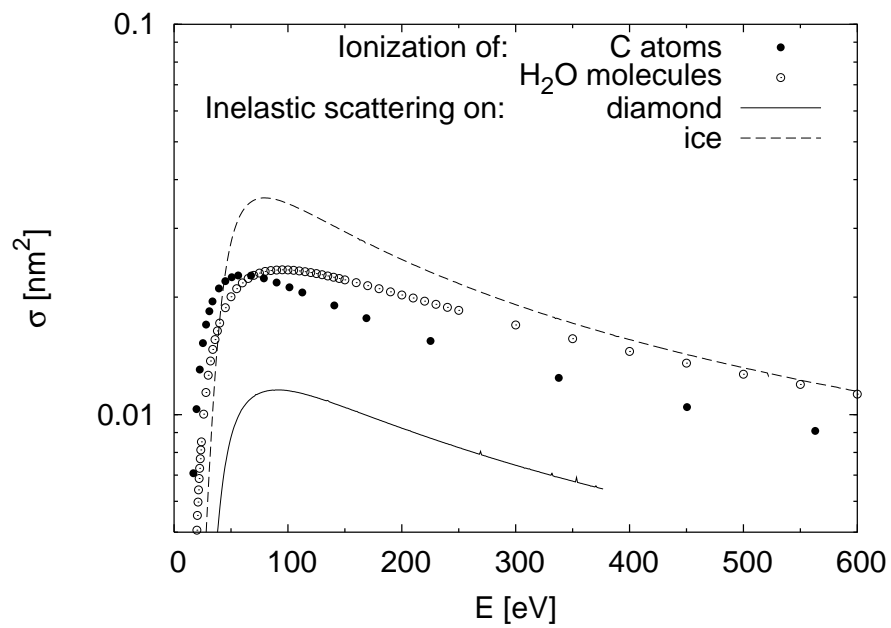


Fig. 4. Timneanu et al.

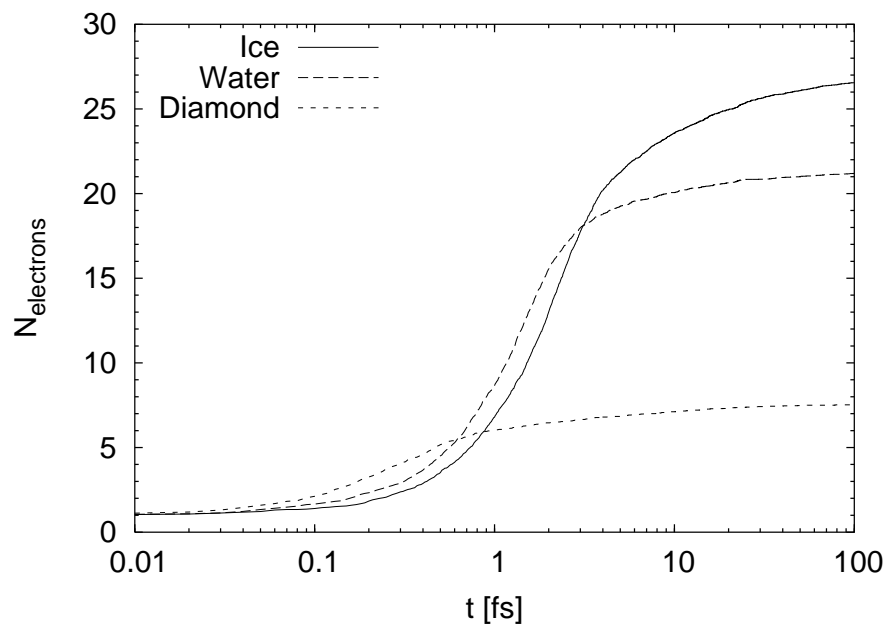


Fig. 5. Timneanu et al.

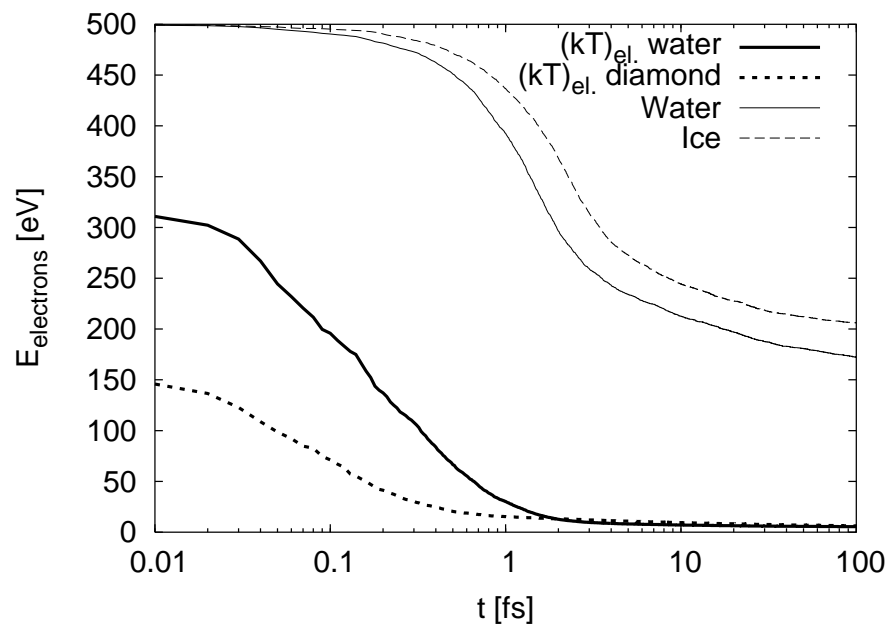


Fig. 6. Timneanu et al.

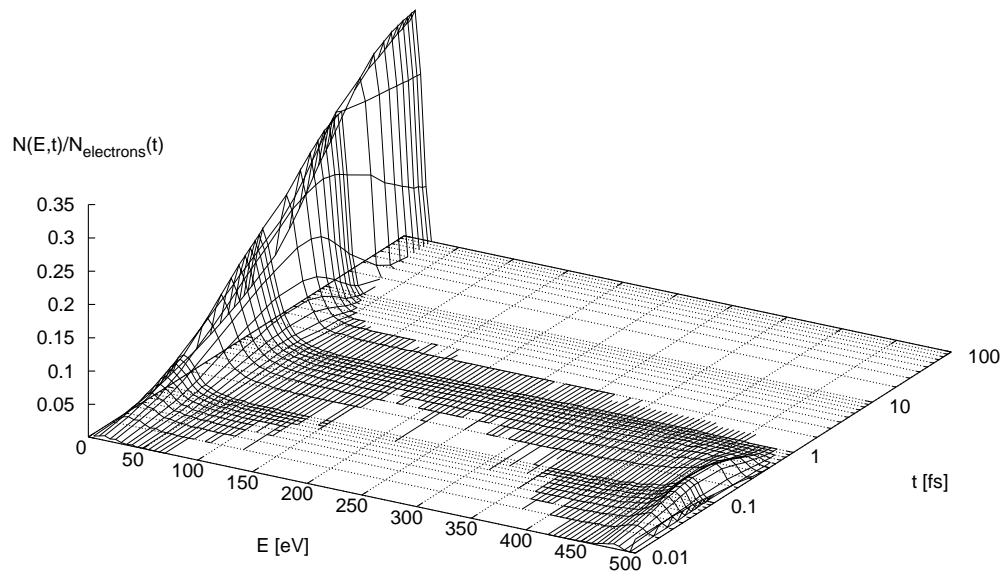


Fig. 7. Timneanu et al.

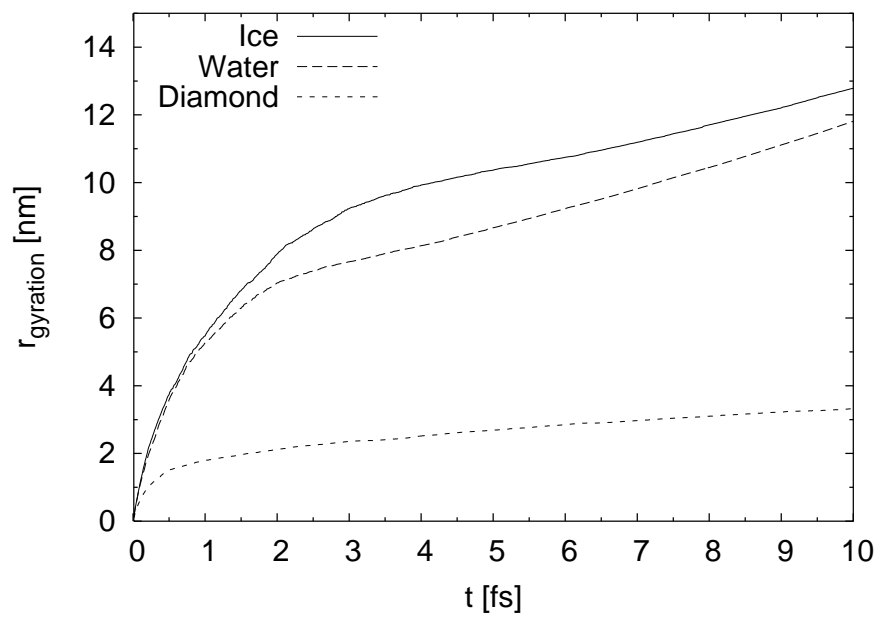


Fig. 8. Timneanu et al.